Article:
Guo, Y., Jin, J., Wang, Q. et al. (2 more authors) (2022) Position-enAbled Complex Toeplitz LISTA for DOA Estimation with Unknow Mutual Coupling. Signal Processing, 194. 108422. ISSN 0165-1684

https://doi.org/10.1016/j.sigpro.2021.108422

Position-Enabled Complex Toeplitz LISTA for DOA Estimation with Unknow Mutual Coupling

Yuzhang Guo[a], Jie Jin[a], Qing Wang[a,*], Hua Chen[b,], Wei Liu[c,]

[a] *School of Electrical and Information Engineering, Tianjin University, Tianjin 300072, China*

[b] *Faculty of Electrical Engineering and Computer Science, Ningbo University, Ningbo, 315211, China*

[c] *Department of Electronic and Electrical Engineering, University of Sheffield, Sheffield S1 3JD, UK*

Abstract

Unfolding iterative algorithms into deep networks can increase the rate of convergence which is amenable to Direction-of-arrival (DOA) estimation problems. However, there normally exists unknown mutual coupling between antenna array elements. In this paper, a novel Position-enAbled Complex Toeplitz Learned Iterative Shrinkage Thresholding Algorithm (PACT-LISTA) is proposed which makes use of the data driven method to solve the mutual coupling effect and improve the parameter estimation performance. First, a sparse recovery (SR) model is developed to explore the inherent Topelitz structure. In order to solve the SR problem, a Complex Toeplitz LISTA (CT-LISTA) network is proposed, which integrates the Toeplitz structure into the Complex LISTA (C-LISTA) network. By ignoring the amplitude and phase information of the recovered signal, the idea of position-priority is applied to further improve the estimation accuracy. Through an innovative iteration method, the system gradually converges to the optimized stable state, which is associated with an accuracy parameter. Simulations are provided to demonstrate that the proposed approach significantly outperforms the state of art methods.

Keywords: DOA estimation, LISTA, complex neural network, sparse

*Corresponding author at: School of Electrical and Information Engineering, Tianjin University, No.92 Weijin Rd, Tianjin 300072, PR China

Email address: wangq@tju.edu.cn (Qing Wang)

recovery, Mutual Coupling

1. Introduction

DOA estimation plays an important role in medical imaging, wireless communications, radar, sonar and navigation. The traditional subspace based methods, such as the multiple signal classification (MUSIC) algorithm [1] and the estimation of signal parameters via rotational invariance techniques (ESPRIT) algorithm[2], [3], require multiple snapshots for covariance estimation. In contrast, the compressed sensing (CS) based method allows recovery of signals in a sparse domain using a small number of snapshots, and can be solved efficiently using the Alternating Direction Method of Multipliers (ADMM) [4] algorithm and the Iterative Shrinkage Thresholding Algorithm (ISTA) [5].

Recently, some deep learning methods, such as spatial distribution feature learning [6] and Deep Neural Networks (DNN) based DOA estimation schemes [7–10], were proposed for effective DOA estimation. By unfolding the ADMM or ISTA algorithms into deep neural networks, several deep unfolding methods [11–14] were proposed to further reduce the number of iterations and accelerate the convergence speed. The learning iterative shrinkage thresholding algorithm (LISTA) [11] is a representative example, which creates a recurrent neural network (RNN) structure to recover sparse signals. In [15], Fu et al proposed a complex-valued convolutional network, named LISTA-Toeplitz, for DOA estimation, where the learned mutual inhibition matrix (MIM) has a Toeplitz structure. These deep unfolding methods outperforms traditional CS based methods in convergence speed and achieves high accuracy in DOA estimation.

For the DOA estimation problem with unknown mutual coupling, the effect of mutual coupling embodied in array manifolds will reduce the parameter estimation accuracy. By adding an auxiliary sensor, the mutual coupling matrix (MCM) can be modeled and converted into a banded symmetric Toeplitz matrix [16], and then CS based sparse recovery (SR) methods can be applied to solve the DOA estimation problem using on-grid [17], off-grid [18] or gridless [19] methods. In this paper, we try to improve the performance of DOA estimation in the presence of unknown mutual coupling by algorithm unfolding. Although MCM breaks the original Toeplitz structure of the MIM by utilizing the special banded symmetric Toeplitz structure of

the MCM of a uniform linear array (ULA) [20] and truncating the signal to construct a new array manifold, we can reconstruct the MIM with a Teoplitz structure.

Furthermore, it is noticed that the SR method can recover both amplitude and phase of the sparse signal, while for DOA estimation, only sparse peak positions are needed in the recovered signal. Inspired by [21], a novel neural network named Position-enAbled Complex Toeplitz LISTA is proposed in this paper, which can directly find the non-zero positions of sparse signals to realize DOA estimation without completely recovering the whole signal.

The paper is organized as follows. Section II introduces the signal model with array mutual coupling and formulation for the DOA estimation problem. Section III proposes a modified neural network which has a better performance in DOA estimation while dealing with mutual coupling effects. A novel neural network is proposed in Section IV to find the non-zero positions of sparse signals to realize DOA estimation. Simulation results are provided in Section V, which show that the proposed networks can deal with the mutual coupling effect effectively and achieve high estimation accuracy with fast convergence rate. Finally, conclusions are drawn in Section VI.

2. Signal Model and Problem Formulation

2.1. Signal Model

Consider a ULA with N elements, and S narrow-band far-field signals $x_s(t),\ s = 1, 2, ..., S$, from directions $\theta_{\mathbf{s}}$= [θ_1,θ_2,$\cdots$,θ_S] respectively. Then, we can have the following data model

$$\mathbf{y}(t) = \mathbf{A}(\theta_{\mathbf{s}})\mathbf{x}_{\mathbf{s}}(t) + \mathbf{n}(t), \tag{1}$$

where $\mathbf{x}_{\mathbf{s}}(t) = [x_1(t), x_2(t), ..., x_S(t)]^T$, $\mathbf{y}(t) = [y_1(t), y_2(t), \ldots, y_N(t)]^T$ denotes the N received signals by the ULA, and $\mathbf{n}(t) = [n_1(t), n_2(t), \ldots, n_N(t)]^T$ is the additive white Gaussian noise vector with zero mean and variance σ_n^2. $\mathbf{A}(\theta_{\mathbf{s}}) = [\mathbf{a}(\theta_1), \mathbf{a}(\theta_2), \ldots, \mathbf{a}(\theta_S)] \in \mathbb{C}^{N\times S}$ is the array steering matrix where $\mathbf{a}(\theta_s) = [a(\theta_s)^0, a(\theta_s)^1, \ldots, a(\theta_s)^{N-1}]^T$ with $a(\theta_s) = e^{-j2\pi\frac{d\sin\theta_s}{\lambda}}$. The spacing between two adjacent array elements is half the signal wavelength λ. By discretizing the whole spatial direction range into K grids ($K >> S$), the received signal vector of the array at snapshot t can be reformulated as

$$\mathbf{y}(t) = \mathbf{A}(\theta)\mathbf{x}(t) + \mathbf{n}(t), \tag{2}$$

where $\theta = [\theta_1, \theta_2, \cdots, \theta_K]$, $\mathbf{x}(t) = [x_1(t), x_2(t), ..., x_K(t)]^T$ is a S-sparse vector, the index of S non-zero elements represents the direction of signals while the other $(K - S)$ zero elements mean that there are no sources to be detected in these directions.

Define $f_s = \frac{1+\sin\theta_s}{2} \in [0, 1]$ as the spatial frequency when $\theta_s \in [-\frac{\pi}{2}, \frac{\pi}{2}]$. The array steering matrix is reformulated as $\mathbf{A} = [\mathbf{a}(f_1), \mathbf{a}(f_2), \ldots, \mathbf{a}(f_K)]$, and the array steering vector $\mathbf{a}(f_s) = [a(f_s)^0, a(f_s)^1, \ldots, a(f_s)^{N-1}]^T$ with $a(f_s) = e^{-j\pi(2f_s-1)}$.

Considering the effect of mutual coupling between adjacent sensors, MCM is introduced and the array outputs are rewritten as

$$\mathbf{M} = \begin{pmatrix} m_0 & m_1 & \cdots & m_{P-1} & & & & & \\ m_1 & m_0 & m_1 & \cdots & m_{P-1} & & \mathbf{0} & & \\ \vdots & \ddots & \ddots & \ddots & \ddots & \ddots & & & \\ m_{P-1} & \cdots & m_1 & m_0 & m_1 & \cdots & m_{P-1} & & \\ & \ddots & \vdots & \ddots & \ddots & \ddots & \ddots & \ddots & \\ & & m_{P-1} & \vdots & m_1 & m_0 & m_1 & \cdots & m_{P-1} \\ & \mathbf{0} & & \ddots & \vdots & \ddots & \ddots & \ddots & \vdots \\ & & & & m_{P-1} & \cdots & m_1 & m_0 & m_1 \\ & & & & & m_{P-1} & \cdots & m_1 & m_0 \end{pmatrix}_{N\times N}, \quad (3)$$

where $m_p, p = 0, \ldots, P-1$, is the mutual coupling coefficient between the n-th sensor and the $(n-p)$-th sensor or $(n+p)$-th sensor with $n = 1, \ldots, N$. As the mutual coupling effect decreases with increasing distance between sensors, we have $m_0 > m_1 > \cdots > m_{P-1}$. The mutual coupling effect between sensors too far apart is ignored.

In order to utilize the Toeplitz structure of the central columns in $\mathbf{M}$, we define a selecting matrix $\mathbf{Q} = [\mathbf{0}_{[N-2(P-1)]\times(P-1)}\ \mathbf{I}_{N-2(P-1)}\ \mathbf{0}_{[N-2(P-1)]\times(P-1)}]$ to establish a new truncated signal as

$$\begin{aligned} \bar{\mathbf{y}}(t) &= \mathbf{Q}\mathbf{y}(t) = \mathbf{Q}\mathbf{M}\mathbf{A}\mathbf{x}(t) + \mathbf{Q}\mathbf{n}(t) \\ &= \bar{\mathbf{M}}\mathbf{A}\mathbf{x}(t) + \mathbf{Q}\mathbf{n}(t), \end{aligned} \quad (4)$$

where $\bar{\mathbf{M}} = \mathbf{Q}\mathbf{M}$ is the central part of $\mathbf{M}$ as

$$\bar{\mathbf{M}} = \begin{bmatrix} m_{P-1} & \cdots & m_1 & m_0 & m_1 & \cdots & m_{P-1} & 0 & 0 \\ 0 & \ddots & \vdots & \ddots & \ddots & \ddots & \ddots & \ddots & 0 \\ 0 & 0 & m_{P-1} & \cdots & m_1 & m_0 & m_1 & \cdots & m_{P-1} \end{bmatrix}_{[N-2(P-1)]\times N}. \quad (5)$$

Then, a new truncated steering vector $\tilde{\mathbf{a}}(f_s)$ considering the effect of mutual coupling can be obtained as

$$\tilde{\mathbf{a}}(f_s) = \bar{\mathbf{M}}\mathbf{a}(f_s) = G(f_s)\bar{\mathbf{a}}(f_s), \tag{6}$$

where $\bar{\mathbf{a}}(f_s) = [a(f_s)^0, a(f_s)^1, ..., a(f_s)^{N-2P+1}]^T$ and $G(f_s) = \sum_{l=1-P}^{P-1} m_{|l|} a(f_s)^{l+P-1}$ is a scalar related to the steering vector and mutual coupling effect. In general, $G(f_s) \neq 0, f_s \in [0, 1]$. Then, $\tilde{\mathbf{a}}(f_s)$ can be reformulated as

$$\tilde{\mathbf{a}}(f_s) = \bar{\mathbf{a}}(f_s)G(f_s). \tag{7}$$

Thus, (4) can be rewritten as

$$\bar{\mathbf{y}}(t) = \bar{\mathbf{A}}\mathbf{H}\mathbf{x}(t) + \mathbf{Q}\mathbf{n}(t), \tag{8}$$

where

$$\mathbf{H} = \begin{bmatrix} G(f_1) & & & 0 \\ & G(f_1) & & \\ & & \ddots & \\ 0 & & & G(f_K) \end{bmatrix} \in \mathbb{C}^{K\times K}, \tag{9}$$

$$\bar{\mathbf{A}} = [\bar{\mathbf{a}}(f_1), \bar{\mathbf{a}}(f_2), ..., \bar{\mathbf{a}}(f_K)] \in \mathbb{C}^{[N-2(P-1)]\times K}. \tag{10}$$

Finally, we establish a new received signal model containing a new target signal $\bar{\mathbf{x}}(t) = \mathbf{H}\mathbf{x}(t)$ as

$$\bar{\mathbf{y}}(t) = \bar{\mathbf{A}}\bar{\mathbf{x}}(t) + \mathbf{Q}\mathbf{n}(t). \tag{11}$$

As $\mathbf{H}$ has a diagonal structure, the results of DOA estimation will be the same by reconstructing $\bar{\mathbf{x}}(t)$ and $\mathbf{x}(t)$ from (11) and (4), respectively.

2.2. Problem Formulation

The DOA estimation problem with unknown mutual coupling can be formulated as a sparse recovery problem as

$$\min_{\bar{\mathbf{x}}(t)} \frac{1}{2} \left\| \bar{\mathbf{y}}(t) - \bar{\mathbf{A}}\bar{\mathbf{x}}(t) \right\|_2^2 + u \left\| \bar{\mathbf{x}}(t) \right\|_1, \tag{12}$$

where $||.||_1$ and $||.||_2$ represents $l_1 norm$ and $l_2 norm$, respectively, and u is a regularization parameter.

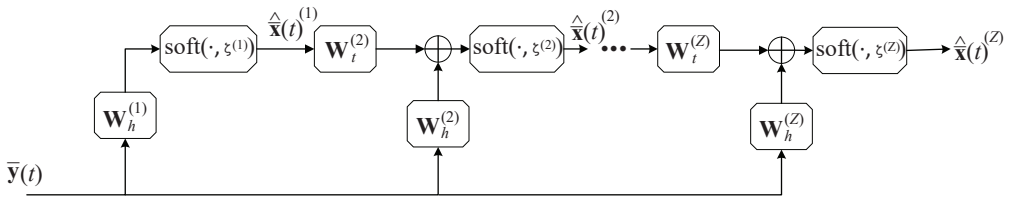

Figure 1: A Z-layer feed-forward LISTA network.

ISTA [5] can be used to recover the sparse signal $\bar{\mathbf{x}}(t)$ iteratively through a recursive formula

$$[\bar{\mathbf{x}}(t)^{k+1}]_i = \text{soft}([\tfrac{1}{L}\bar{\mathbf{A}}^H\bar{\mathbf{y}}(t) + (\mathbf{I} - \tfrac{1}{L}\bar{\mathbf{A}}^H\bar{\mathbf{A}})\bar{\mathbf{x}}(t)^k]_i, \tfrac{u}{L}) \ , \tag{13}$$

where $\text{soft}(\omega_i, \varepsilon) \doteq \text{sign}(\omega_i)\max(|\omega_i| - \varepsilon, 0)$, L is the Lipschitz constant, k is the index of iteration, and $[\bar{\mathbf{x}}(t)]_i$ is the i-th element of vector $\bar{\mathbf{x}}(t)$.

Our problem is to unfold the ISTA algorithm in (13) into a deep neural network to improve the estimation accuracy and accelerate the convergence speed. Specifically, for DOA estimation, we would like to design a neural network for complex signal processing and make full use of the inherent signal structure.

3. Proposed Complex Toeplitz LISTA Network for DOA Estimation with Uknown Mutual Coupling

The learned iterative shrinkage and thresholding algorithm (LISTA) [22] is a recurrent neural network designed to mimic ISTA for approximating the solution of (13). An example Z-layer feed-forward LISTA network is shown in Fig. 1.

For the DOA estimation problem in (13), the output of the $(k+1)$-th layer of the LISTA network is given by

$$\bar{\mathbf{x}}(t)^{(k+1)} = \text{soft}(\mathbf{W}_h{}^{(k)}\bar{\mathbf{y}}(t) + \mathbf{W}_t{}^{(k)}\bar{\mathbf{x}}(t)^{(k)}, \zeta^{(k)}), \tag{14}$$

where k represents the network layer index ranging from 0 to $Z-1$, $\mathbf{W}_h$ and $\mathbf{W}_t$ are the filter matrix and the mutual inhibition matrix (MIM), respectively. These two matrices are initialized to $\mathbf{W}_h = \frac{1}{L}\bar{\mathbf{A}}^H$ and $\mathbf{W}_t = \mathbf{I} - \frac{1}{L}\bar{\mathbf{A}}^{\mathbf{H}}\bar{\mathbf{A}}$ at each layer, while $\zeta = \frac{u}{L}$ is the soft threshold initialization value, and

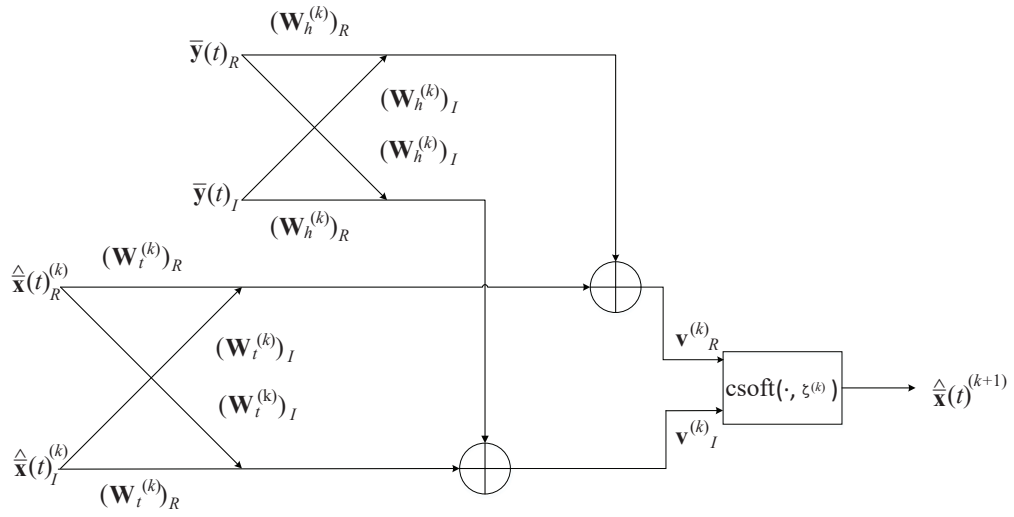

Figure 2: One layer of the Complex LISTA Network.

$\mathbf{\Theta}^{(k)} = [\mathbf{W}_h{}^{(k)}, \mathbf{W}_t{}^{(k)}, \zeta^{(k)}]$ is the parameters to be learned. $\mathbf{\Theta}^{(k)}$ is learned during the training phase by minimizing the quadratic loss function

$$L(\mathbf{\Theta}^{(k)}) = \frac{1}{J}\sum_{j=1}^{J}\left\|\hat{\bar{\mathbf{x}}}(t)^{j,(k)}\left(\bar{\mathbf{y}}(t)^j;\mathbf{\Theta}^{(k)}\right) - \bar{\mathbf{x}}(t)^j\right\|_2^2, \tag{15}$$

where J is the number of samples in the training data set, and $\hat{\mathbf{x}}(t)^{(k)}\left(\bar{\mathbf{y}}(t)^j;\mathbf{\Theta}^{(k)}\right)$ is the output of the k-th layer network using input $\bar{\mathbf{y}}(t)^j$ and parameters $\mathbf{\Theta}^{(k)}$. This learning based method requires no prior information of array manifold at the training phase; however, such information can be used at the initiation phase only.

3.1. Complex LISTA Network

Most popular deep learning toolboxes, such as Tensorflow and Pytorch, are designed for real-valued signals, which is not directly applicable to DOA estimation problems. Separating the training data into real and imaginary parts using two channels will double the network size and break the connection between them, thus losing the amplitude and phase information of the complex numbers.

To this end, a new Complex LISTA (C-LISTA) network is proposed to deal with the complex-valued data, which provides a nested structure of input

and output data at each layer, as shown in Fig. 2. The real and imaginary parts are represented by $(\cdot)_R$ and $(\cdot)_I$, respectively, and the output of the k-th network is

$$\bar{\mathbf{x}}(t)^{(k+1)} = \text{csoft}(\mathbf{v}^{(k)}{}_R + \mathbf{v}^{(k)}{}_I\sqrt{-1}, \zeta^{(k)}), \tag{16}$$

where

$$\begin{aligned} \mathbf{v}^{(k)}{}_R &= (\mathbf{W}_h{}^{(k)})_R\bar{\mathbf{y}}(t)_R + (\mathbf{W}_t{}^{(k)})_R(\bar{\mathbf{x}}(t)^{(k)})_R \\ &\quad -(\mathbf{W}_h{}^{(k)})_I\bar{\mathbf{y}}(t)_I - (\mathbf{W}_t{}^{(k)})_I(\bar{\mathbf{x}}(t)^{(k)})_I, \\ \mathbf{v}^{(k)}{}_I &= (\mathbf{W}_h{}^{(k)})_R\bar{\mathbf{y}}(t)_I + (\mathbf{W}_t{}^{(k)})_R(\bar{\mathbf{x}}(t)^{(k)})_I \\ &\quad +(\mathbf{W}_h{}^{(k)})_I\bar{\mathbf{y}}(t)_R + (\mathbf{W}_t{}^{(k)})_I(\bar{\mathbf{x}}(t)^{(k)})_R, \end{aligned} \tag{17}$$

$\sqrt{-1}$ is the imaginary unit. Let $\mathbf{v} = \mathbf{v}_R + \mathbf{v}_I\sqrt{-1} \in \mathbb{C}^K$, a complex soft threshold operator $\text{csoft}(\cdot, \zeta)$ is proposed to replace the soft threshold operator in (14), that is

$$\text{csoft}(\mathbf{v},\zeta)_i = \mathbf{v}_i\frac{\max(|\mathbf{v}_i| - \zeta, 0)}{\max(|\mathbf{v}_i| - \zeta, 0) + \zeta}, \quad i = 1, 2, \cdots, K. \tag{18}$$

The loss function in (15) is reformulated to the complex form as

$$L(\mathbf{\Theta}^{(k)}) = \frac{1}{2J}\sum_{j=1}^{J}\left(\begin{array}{l} \left\| \hat{\bar{\mathbf{x}}}(t)_R^{(k)}\left(\bar{\mathbf{y}}(t)_R{}^j; \mathbf{\Theta}^{(k)}\right) - \bar{\mathbf{x}}(t)_R{}^j \right\|_2 + \\ \left\| \hat{\bar{\mathbf{x}}}(t)_I{}^{(k)}\left(\bar{\mathbf{y}}(t)_I{}^j; \mathbf{\Theta}^{(k)}\right) - \bar{\mathbf{x}}(t)_I{}^j \right\|_2 \end{array} \right). \tag{19}$$

3.2. Complex Toeplitz LISTA Network

As for DOA estimation, the initialization of MIM $\mathbf{I} - \frac{1}{L}\bar{\mathbf{A}}^H\bar{\mathbf{A}}$ of LISTA network in (14) ought to be a Toeplitz matrix, as $\bar{\mathbf{A}}^H\bar{\mathbf{A}}$ is a Gram matrix whose element at the i-th row and j-th column $[\bar{\mathbf{A}}^H\bar{\mathbf{A}}]_{ij} = \bar{\mathbf{a}}(f_i)^H\bar{\mathbf{a}}(f_j)$, which means that it might be able to shrink the unfolded network by reducing the dimensionality of MIMs. Accordingly, the matrix multiplication $\mathbf{W}_t\bar{\mathbf{x}}(t)$ can be transformed into vector convolution $\mathbf{c}_t * \bar{\mathbf{x}}(t)$, formulated as

$$\mathbf{W}_t\bar{\mathbf{x}}(t) = \mathbf{c}_t * \bar{\mathbf{x}}(t), \tag{20}$$

where

$$\mathbf{W}_t = \begin{bmatrix} c_0 & c_{-1} & c_{-2} & \cdots & c_{-(K-1)} \\ c_1 & c_0 & c_{-1} & \ddots & \vdots \\ c_2 & \ddots & \ddots & \ddots & c_{-2} \\ \vdots & \ddots & \ddots & \ddots & c_{-1} \\ c_{K-1} & \cdots & c_2 & c_1 & c_0 \end{bmatrix}, \tag{21}$$

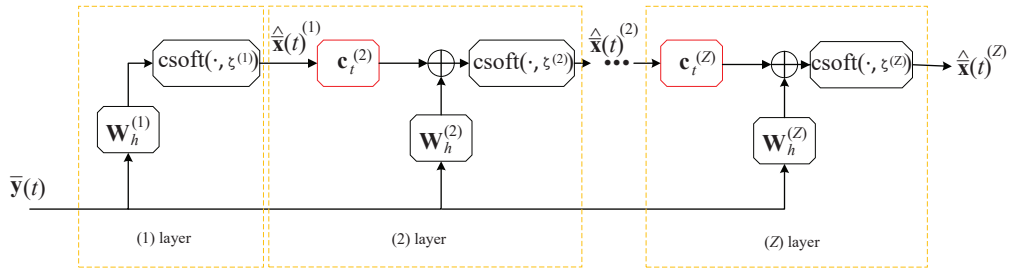

Figure 3: Complex Toeplitz LISTA Network.

$$\mathbf{c}_t = [c_{-(K-1)}, ..., c_{-1}, c_0, c_1, ..., c_{K-1}]^T. \tag{22}$$

By applying the the convolutional operation, we propose a new network called Complex Toeplitz LISTA (CT-LISTA), as shown in Fig. 3. $\mathbf{\Theta}_c{}^{(k)} = [\mathbf{W}_h{}^{(k)}, \mathbf{c}_t{}^{(k)}, \zeta^{(k)}]$ is considered as the network parameters to be learned. Each layer is constructed by a linear convolutional operator with a proximal mapping and the output of the $(k-1)$-th layer. The two-dimensional learnable weight matrix $\mathbf{W}_t{}^{(k)}$ of size $K \times K$ is transformed into a one-dimensional weight vector $\mathbf{c}_t$ of size $2K1$ by modifying (17) into

$$\begin{aligned} \mathbf{v}^{(k)}{}_R &= (\mathbf{W}_h{}^{(k)})_R \bar{\mathbf{y}}(t)_R + (\mathbf{c}_t{}^{(k)})_R * (\bar{\mathbf{x}}(t)^{(k)})_R \\ &\quad -(\mathbf{W}_h{}^{(k)})_I \bar{\mathbf{y}}(t)_I - (\mathbf{c}_t{}^{(k)})_I * (\bar{\mathbf{x}}(t)^{(k)})_I, \\ \mathbf{v}^{(k)}{}_I &= (\mathbf{W}_h{}^{(k)})_R \bar{\mathbf{y}}(t)_I + (\mathbf{c}_t{}^{(k)})_R * (\bar{\mathbf{x}}(t)^{(k)})_I \\ &\quad +(\mathbf{W}_h{}^{(k)})_I \bar{\mathbf{y}}(t)_R + (\mathbf{c}_t{}^{(k)})_I * (\bar{\mathbf{x}}(t)^{(k)})_R. \end{aligned} \tag{23}$$

Therefore, the proposed CT-LISTA network greatly reduces the number of weight units required for training compared with the other LISTA networks, and will be able to deal with large-scale sparse recovery problems more efficiently. In addition, by making full use of the inherent data structure the estimation accuracy can be improved potentially.

4. Proposed Improved Position-enAbled Network

The above CT-LISTA network reconstructs the target signal $\hat{\bar{\mathbf{x}}}$ firstly and then determines the target direction based on position of the non-zero elements of the reconstructed signal. Considering the amplitude of $\hat{\bar{\mathbf{x}}}(t)$ is not required for DOA estimation, in this section, we propose a Position-enAbled Complex Toeplitz LISTA (PACT-LISTA) network which is specifically designed for DOA estimation and does not need to reconstruct the signal in advance, as shown in Fig. 4.

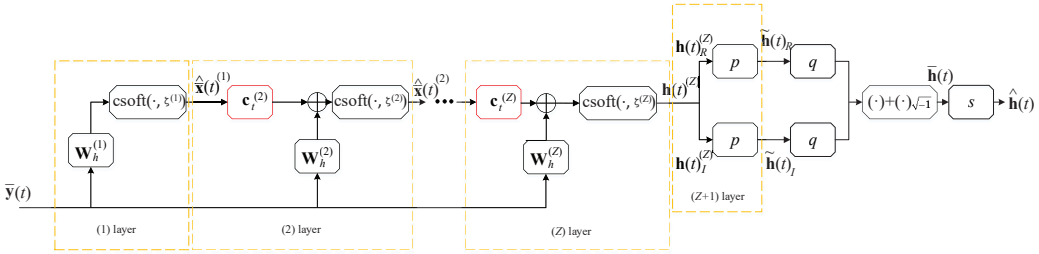

Figure 4: Z-layer Position-enAbled Complex Toeplitz LISTA Network.

Firstly, we modify the training data set from $\{(\bar{\mathbf{y}}(t)^j, \bar{\mathbf{x}}(t)^j)\}_{j=1}^J$ to $\{(\bar{\mathbf{y}}(t)^j, \mathbf{h}(t)^j)\}_{j=1}^J$ by defining the *position-enabled labels* $\mathbf{h}(t)^j$ as

$$[\mathbf{h}(t)^j]_l = \begin{cases} 1+\sqrt{-1}, & \text{if } [\bar{\mathbf{x}}(t)^j]_l \neq 0, \\ 0, & \text{otherwise} \end{cases}. \tag{24}$$

In order to limit the real and imaginary parts of output in the Z-th layer, i.e., $\left(\mathbf{h}(t)^{(Z)}\right)_R$ and $\left(\mathbf{h}(t)^{(Z)}\right)_I$, to the range of $[0,1]$, so that it can be compared with the revised position-enabled labels $\mathbf{h}(t)^j$, we define a bounded function as

$$p(h) = |\tanh(h)| = \left|\frac{e^h - e^{-h}}{e^h + e^{-h}}\right|. \tag{25}$$

Then, the output p is binarized into 0 and 1 using the unit step function

$$q(p) = \varepsilon(p-\xi) = \begin{cases} 1, & p \geq \xi \\ 0, & p < \xi \end{cases}. \tag{26}$$

As the binary function is non-differential, we train the neural network using the output of $p(\cdot)$ rather than $q(\cdot)$. The loss function is defined as

$$L(\boldsymbol{\Theta}_c{}^{(k)}) = \frac{1}{2J}\sum_{j=1}^{J}\left(\begin{array}{l} \left\|\widetilde{\mathbf{h}}(t)_R{}^{(k)}\left(\bar{\mathbf{y}}(t)_R{}^j; \boldsymbol{\Theta}_c{}^{(k)}\right) - \mathbf{h}(t)_R{}^j\right\|_2 + \\ \left\|\widetilde{\mathbf{h}}(t)_I{}^{(k)}\left(\bar{\mathbf{y}}(t)_I{}^j; \boldsymbol{\Theta}_c{}^{(k)}\right) - \mathbf{h}(t)_I{}^j\right\|_2 \end{array}\right). \tag{27}$$

By combining the real and image channels, it can be seen that the resulting complex output $\bar{\mathbf{h}}(t)$ contains the values $\sqrt{-1}$ and 1, which are not required and should be removed using the selection function

$$s(\bar{h}) = \begin{cases} 1+\sqrt{-1}, & |\bar{h}| > 1 \\ 0, & \text{else} \end{cases}. \tag{29}$$

Finally, $\hat{\mathbf{h}}(t)$ is estimated in terms of non-zero tap positions of $\bar{\mathbf{x}}(t)$, i.e., $[\hat{\mathbf{h}}(t)]_l = 0$ or $[\hat{\mathbf{h}}(t)]_l = 1 + \sqrt{-1}$, corresponding to the taps of the reconstructed signal $\hat{\mathbf{x}}(t)$ in Section III with zero value or non-zero value, respectively.

5. SIMULATION RESULTS

In this section, simulations are performed to show the effectiveness of the proposed CT-LISTA and PACT-LISTA. Two other methods, including ISTA and LISTA are considered for performance comparison.

The normalized mean squared error (NMSE)

$$NMSE = \frac{1}{SD_{test}} \sum_{s=1}^{S} \sum_{j=1}^{D_{test}} \left(f_s^{(j)} - \hat{f}_s^{(j)} \right)^2, \tag{30}$$

is used as performance metric when the number of target sources is known. D_{test} is the size of the test set.

However, the NMSE metric is no longer suitable when the number of target sources is unknown because we can not guarantee the equal size of $\hat{\mathbf{f}}_\mathbf{s}$ and $\mathbf{f}_\mathbf{s}$. To this end, we resort to a new metric called Hausdorff distance [23]. For two sets $\mathcal{A}$ and $\mathcal{B}$ of all the members of vectors $\hat{\mathbf{f}}_\mathbf{s}$ and $\mathbf{f}_\mathbf{s}$, respectively, the Hausdorff distance is defined as

$$d_H(\mathcal{A}, \mathcal{B}) = \max\{d(\mathcal{A}, \mathcal{B}), d(\mathcal{B}, \mathcal{A})\}, \tag{31}$$

where

$$d(\mathcal{A}, \mathcal{B}) = \sup\{d(\hat{f}_s, \mathcal{B}) | \hat{f}_s \in \mathcal{A}\}, \tag{32}$$

is the directed difference, $d(\hat{f}_s, \mathcal{B}) = \inf\{d(\hat{f}_s, f_s) | f_s \in \mathcal{B}\}$ and $d(\hat{f}_s, f_s) = |\hat{f}_s - f_s|$. For evaluation over the testing set we have used its mean value, denoted as

$$Hd(\mathbf{f}_\mathbf{s}) = \frac{1}{D_{test}} \sum_{j=1}^{D_{test}} d_H((\mathcal{A})^j, (\mathcal{B})^j). \tag{33}$$

5.1. Experimental Setup

Consider an ULA which has $N = 64$ sensors with $S = 5$ far-field narrowband sources arriving at different directions. The whole angle range is uniformly discretized into $K = 180$ points and the number of independent sources is S so that the single-snapshot target signal $\mathbf{x}(t)$ is S-sparse. $P = 4$ and the mutual coupling coefficients are $\mathrm{m}_0 = 1, \mathrm{m}_1 = 0.4864 - 0.4468\sqrt{-1}$, $\mathrm{m}_2 = 0.2545 + 0.2344\sqrt{-1}$ and $\mathrm{m}_3 = 0.1386 - 0.1478\sqrt{-1}$.

5.2. Results and Discussions

5.2.1. CT-LISTA network

We generate two data sets $\{\bar{\mathbf{y}}(t)^j, \bar{\mathbf{x}}(t)^j\}_{j=1}^J$ and $\{\mathbf{y}(t)^j, \mathbf{x}(t)^j\}_{j=1}^J$ according to (2) and (11), with and without the effects of mutual coupling, respectively. The directions of 5 signals are generated randomly with batch size of 1000. The training and the testing data are generated in the same way, while the size of the training set is dependent on the convergence of the loss function or reaching a given maximal number of epochs.

Fig. 5 shows the reconstructed signals $\hat{\mathbf{x}}(t)$ obtained from C-LISTA network and CT-LISTA network supposing this effect does not exist in the measurement data. It can be seen that both neural networks can achieve high-precision DOA estimation under noiseless conditions. Fig. 6 shows the

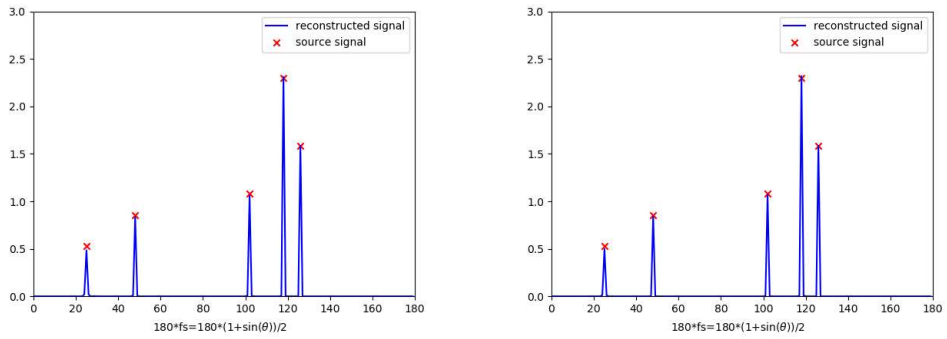

(a) (b)

Figure 5: Network outputs without mutual coupling in the noiseless case: (a) C-LISTA, (b) CT-LISTA.

reconstructed signals $\hat{\mathbf{x}}(t)$ obtained from C-LISTA network and CT-LISTA network considering only the effect of the mutual coupling without the noise. It can be seen that even if the reconstructed signal cannot be close to the source signal $\mathbf{x}(t)$ due to the influence of mutual coupling, DOA estimation can be well realized. When SNR=14dB, the DOA estimation results are shown in Fig. 7. It can be seen that the influence of noise on experimental results is very small compared with that of mutual coupling.

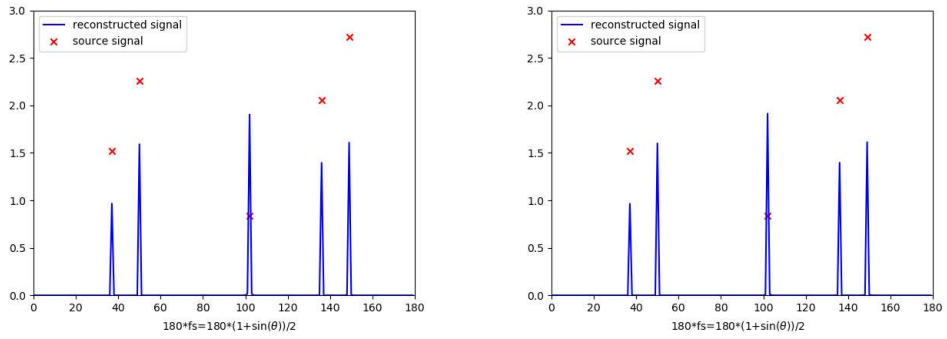

(a) (b)

Figure 6: Network outputs with mutual coupling in the noiseless case. (a) C-LISTA, (b) CT-LISTA

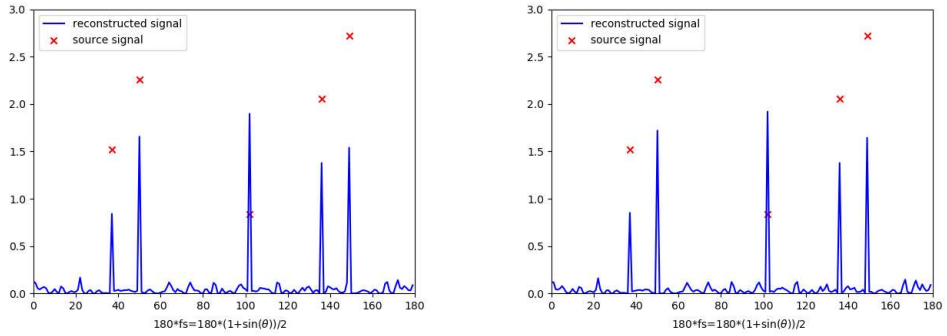

(a) (b)

Figure 7: Network outputs with mutual coupling, SNR=14dB: (a) C-LISTA, (b) CT-LISTA

We analyse the performance of the proposed the CT-LISTA network under different number of arrays. In the high SNR region, the more the number of elements, the better the estimation result in Fig. 8. However, it is not obvious in the low SNR region.

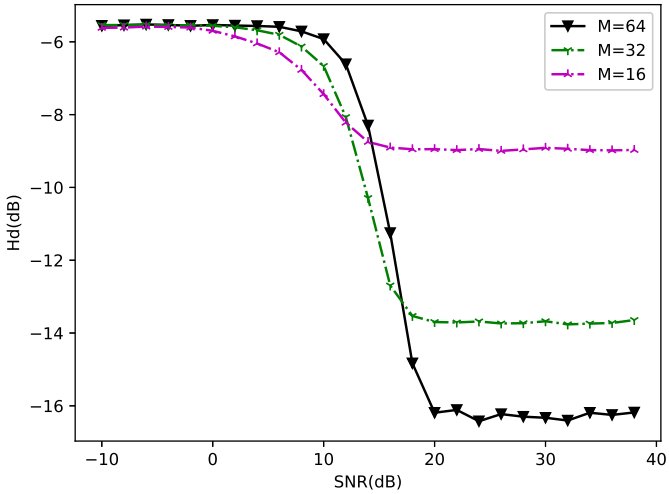

Figure 8: DOA estimation performance under different number of arrays verses SNR (CT-LISTA)

Fig. 9 presents the NMSE and Hd results verse the iteration number in noiseless case, with known and unknown number of sources, respectively, and the maximum number of iterations being 20. DOA estimation results are obtained from indexes of S maximum signal peaks if the number of sources is known, while the crest search method is applied under unknown number of sources situation. ISTA will convergences to about -15dB after 3000 iterations. It can be seen that the neural network methods have a faster convergence speed. On the other hand, it also shows that CT-LISTA further improves the DOA estimation performance compared to C-LISTA.

Fig. 10 shows the performance comparison at different SNRs. It can be seen that the proposed CT-LISTA has the best DOA estimation accuracy compared with other methods in the case of mutual coupling and the neural network methods outperform ISTA. However, all methods fails at the low SNR region, specifically, lower than 10dB.

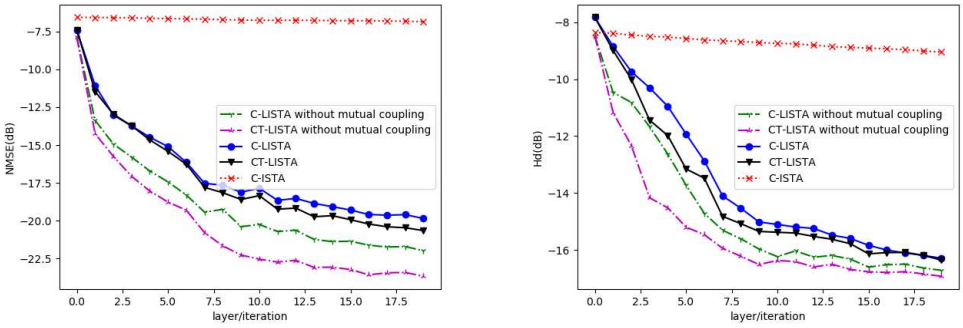

(a) (b)

Figure 9: DOA estimation performance verse layers or iterations in noiseless case: (a) known number of sources, (b) unknown number of sources.

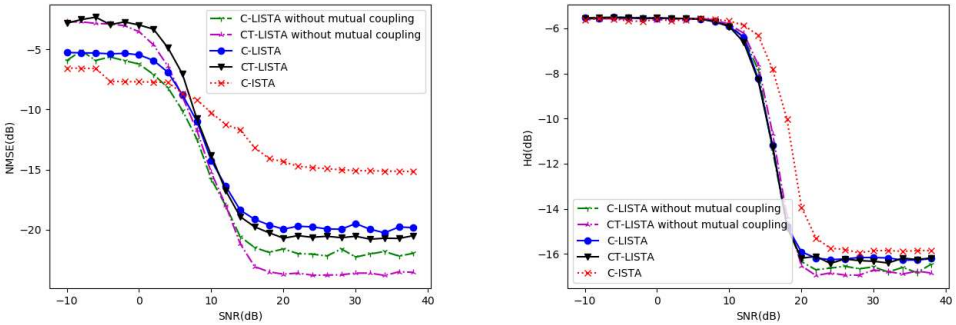

(a) (b)

Figure 10: DOA estimation accuracy verse SNR: (a) known number of sources, (b) unknown number of sources.

5.2.2. PACT-LISTA

The performance of the proposed PACT-LISTA is evaluated in this subsection. The revised position-enabled training data sets $\{\bar{\mathbf{y}}(t)_M^j, \mathbf{h}(t)_M^j\}_{j=1}^J$ and independent testing data sets are generated according to (24). The threshold in (26) is set to $\xi = 0.3$. The neural network is trained by minimizing the loss function (27) using the Adam optimizer.

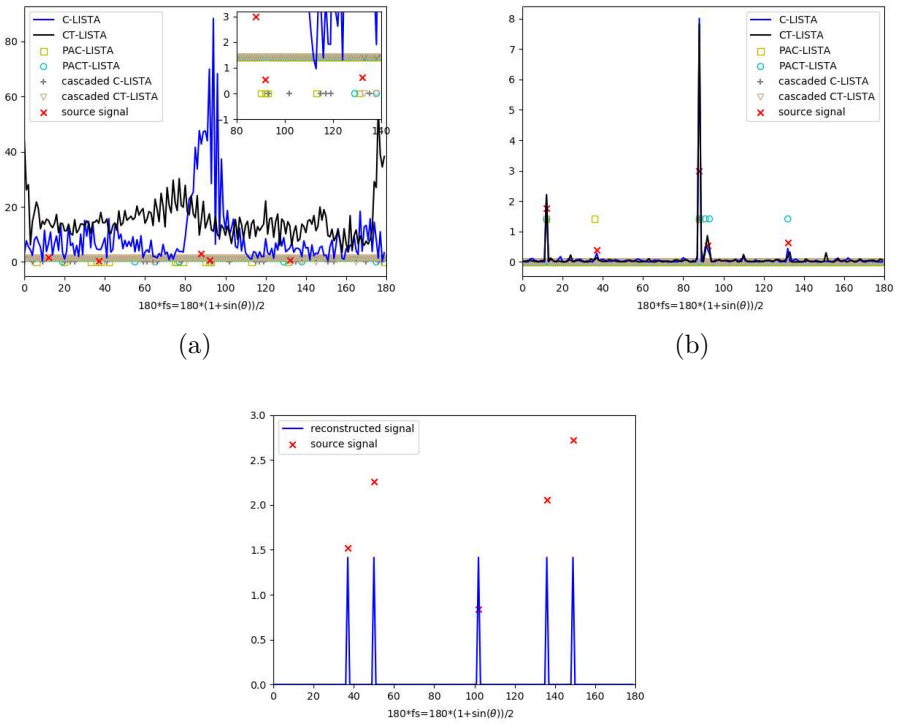

Figure 11: DOA estimation performance with mutual coupling effect and unknown number of sources: (a) SNR=2dB, (b) SNR=12dB, (c) SNR=14dB.

We firstly compare the performance of the proposed PACT-LISTA network, the CT-LISTA network and the CT-LISTA combining (25), (26), (29), namely the cascaded CT-LISTA network. At low SNR region, all methods have failed as no individual peaks can be found in the spectrogram, as shown in Fig. 11(a). As SNR increases, the proposed PACT-LISTA network has outperformed all the other methods, as shown in Fig. 11(b), where the PAC-LISTA missed two signals while the cascaded methods could not capture the weak ones. Compared with CT-LISTA in Fig. 7, it is found that the PACT-LISTA method has removed small peak errors, which can be seen more clearly in Fig. 11(c).

We compare the performance of the proposed PACT-LISTA network and the CT-LISTA network under different number of signal sources. For CT-LISTA, at low SNR region, the more regional signal sources, the better the

estimation effect will be in Fig. 12(a). The reverse is true for high SNR regions. For PACT-LISTA, the experimental estimation results are always better when the number of signal sources is smaller in Fig. 12(b).

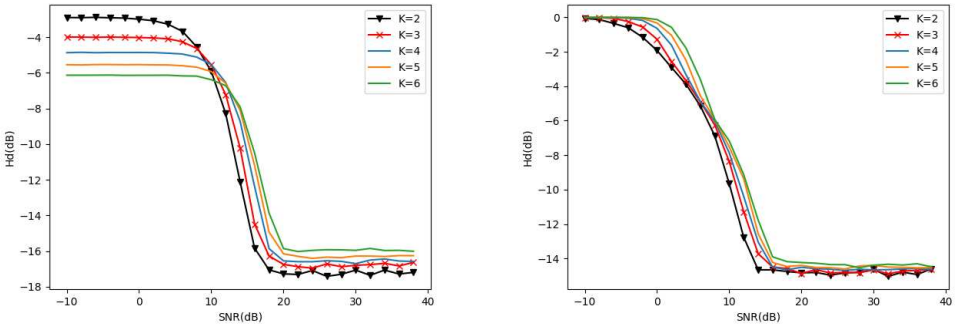

(a) (b)

Figure 12: DOA estimation performance under different number of signal sources verses SNR. (a) CT-LISTA, (b) PACT-LISTA,

When the number of sources is known, we evaluate the DOA estimation performance of the PACT-LISTA network using the NMSE metric, as shown in Fig. 13(a). We can see that CT-LISTA outperforms PACT-LISTA because the sparse recovery method always performs well with knowledge of sparsity degree, which is the number of sources, i.e., number of supports in this problem.

When the number of sources is unknown, at low SNR region, once all the elements in $\hat{\mathbf{h}}(t)$ equal $1+\sqrt{-1}$, it will result into peak crest failure. Thus we have a null set of $\mathcal{A}$ and the Hausdorff distance equals 1 as the maximal value of $f_s = 1$. The advantages of the proposed position-enabled scheme in 8-18dB SNR region have demonstrated that the network focusing on the location of the supports rather than the recovery of the signal itself is proper for DOA estimation problems. When SNR is greater than 18dB, the sparse recovery methods have the best performance.

6. Conclusion

In this paper, two different neural networks have been proposed to realize fast and high-accuracy DOA estimation in the presence of unknown mutual

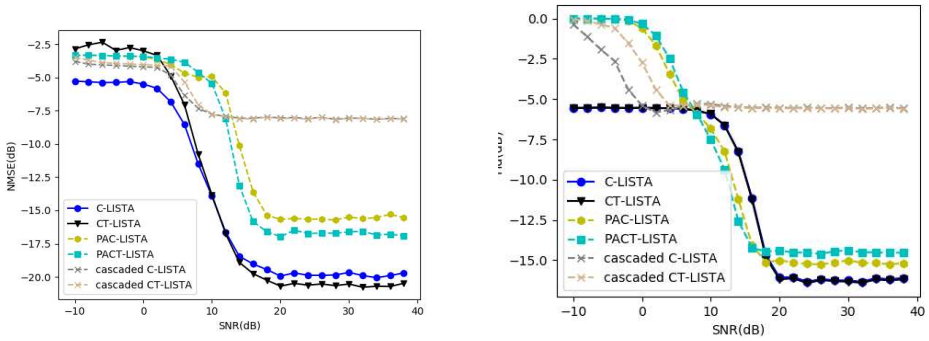

(a) (b)

Figure 13: DOA estimation performance verses SNR: (a) known number of sources, (b) unknown number of sources.

coupling effect. A new signal model is established by processing the received signal and fusing the mutual coupling coefficient with part of the source signals. Then, exploiting the Toeplitz structure of mutual inhibition matrix in LISTA, the CT-LISTA is proposed with a faster convergence speed than ISTA and LISTA. In addition, the CT-LISTA network greatly reduces the number of parameters required for training by reducing the dimension of network variables. To further improve the DOA estimation performance, the PACT-LISTA network is then proposed, which focuses on estimation of the source angles while ignoring the amplitude and phase information of the sources. Simulation results show that the CT-LISTA networks have achieved a better performance in terms of estimation accuracy and convergence speed than LISTA and ISTA, while PACT-LISTA is better than CT-LISTA with unknown number of targets.

Acknowledgment

This work is supported by the National Natural Science Foundation of China (Grants No. 61871282 and 62001256) and the Zhejiang Provincial Natural Science Foundation of China (Grant No. LQ19F010002).

References

[1] R. Schmidt, Multiple emitter location and signal parameter estimation, IEEE Transactions on Antennas and Propagation 34 (1986) 276–280.

[2] R. Roy, T. Kailath, ESPRIT-estimation of signal parameters via rotational invariance techniques, IEEE Transactions on Acoustics, Speech, and Signal Processing 37 (1989) 984–995.

[3] H. Chen, W. Wang, W. Liu, Augmented Quaternion ESPRIT-Type DoA Estimation With a Crossed-Dipole Array, IEEE Communications Letters 24 (2020) 548–552.

[4] S. Boyd, N. Parikh, E. Chu, B. Peleato, J. Eckstein, Distributed optimization and statistical learning via the alternating direction method of multipliers, Foundations and Trends in Machine Learning 3 (2010) 1–122.

[5] A. Beck, M. Teboulle, A fast iterative shrinkage-thresholding algorithm for linear inverse problems, Siam Journal on Imaging Sciences 2 (2009) 183–202.

[6] H. Xiang, B. Chen, H. Xu, Spatial distribution feature learning for doa estimation in multi-path environment, in: IEEE International Conference on Computational Electromagnetics (ICCEM), 2019, pp. 1–4.

[7] H. Huang, G. Gui, H. Sari, F. Adachi, Deep learning for super-resolution doa estimation in massive mimo systems, in: IEEE Vehicular Technology Conference (VTC-Fall), 2018, pp. 1–5.

[8] H. Huang, J. Yang, H. Huang, Y. Song, G. Gui, Deep Learning for Super-Resolution Channel Estimation and DOA Estimation Based Massive MIMO System, IEEE Transactions on Vehicular Technology 67 (2018) 8549–8560.

[9] Z. Liu, C. Zhang, P. S. Yu, Direction-of-arrival estimation based on deep neural networks with robustness to array imperfections, IEEE Transactions on Antennas and Propagation 66 (2018) 7315–7327.

[10] C. Wang, W. Liu, M. Jiang, A unified approach for target direction finding based on convolutional neural networks, in: 2020 IEEE 30th International Workshop on Machine Learning for Signal Processing (MLSP), 2020, pp. 1–6.

[11] H. Sreter, R. Giryes, Learned convolutional sparse coding, in: IEEE International Conference on Acoustics, Speech and Signal Processing (ICASSP), 2018, pp. 2191–2195.

[12] Y. Li, X. Cheng, G. Gui, Co-Robust-ADMM-Net: Joint ADMM Framework and DNN for Robust Sparse Composite regularization, IEEE Access 6 (2018) 47943–47952.

[13] Y. Yang, J. Sun, H. Li, Z. Xu, ADMM-CSNet: A Deep Learning Approach for Image Compressive Sensing, IEEE Transactions on Pattern Analysis and Machine Intelligence 42 (2020) 521–538.

[14] J. Zhang, B. Ghanem, ISTA-Net: Interpretable optimization-inspired deep network for image compressive sensing, in: IEEE/CVF Conference on Computer Vision and Pattern Recognition (CVPR), 2018, pp. 1828–1837.

[15] R. Fu, T. Huang, Y. Liu, Y. C. Eldar, Compressed LISTA exploiting Toeplitz structure, in: IEEE Radar Conference (RadarConf), 2019, pp. 1–6.

[16] T. Svantesson, Modeling and estimation of mutual coupling in a uniform linear array of dipoles, in: IEEE International Conference on Acoustics, Speech, and Signal Processing. Proceedings (ICASSP), 1999, pp. 2961–2964.

[17] Q. Wang, T. Dou, H. Chen, W. Yan, W. Liu, Effective block sparse representation algorithm for doa estimation with unknown mutual coupling, IEEE Communications Letters 21 (2017) 2622–2625.

[18] C. Peng, Z. Cao, Z. Chen, X. Wang, Off-grid DoA estimation using sparse Bayesian learning in MIMO radar with unknown mutual coupling, IEEE Transactions on Signal Processing 67 (2019) 208–220.

[19] Q. Wang, X. Wang, T. Dou, H. Chen, X. Wu, Gridless super-resolution DoA estimation with unknown mutual coupling, in: IEEE International Conference on Acoustics, Speech and Signal Processing (ICASSP), 2019, pp. 4210–4214.

[20] H. Wu, C. Hou, H. Chen, W. Liu, Q. Wang, Direction finding and mutual coupling estimation for uniform rectangular arrays, Signal Processing 117 (2015) 61 – 68.

[21] E. C. Marques, N. Maciel, L. Naviner, H. Cai, J. Yang, Deep learning approaches for sparse recovery in compressive sensing, in: International Symposium on Image and Signal Processing and Analysis (ISPA), 2019, pp. 129–134.

[22] K. Gregor, Y. Lecun, Learning fast approximations of sparse coding, in: International Conference on Machine learning (ICML), 2010, pp. 399–406.

[23] G. Papageorgiou, M. Sellathurai, Y. C. Eldar, Deep networks for direction-of-arrival estimation in low snr, ArXiv abs/2011.08848 (2020).